RESEARCH ARTICLE

Editorial Process: Submission:03/31/2023 Acceptance:07/08/2023

Induction of Apoptosis and Modulation of Caspase Activity on MCF-7 Human Breast Cancer Cells by Bioactive Fractionated Cocoa Leaf Extract

Yazan Ranneh[1]*, Mohd. Fadzelly Abu Bakar[2], Abdah Md Akim[3], Zainal Bin Baharum[3], Mohammed S Ellulu[4], Abdulmannan Fadel[5]

Abstract

Background: The objective of this study was to investigate the potential anti-proliferative activities of a methanolic extract of cocoa leaves (CL) obtained through sequential partition and fractionation against MCF-7 breast cancer cells. **Methods:** The methanolic extract of CL was partitioned in three separated solvents (hexane, dichloromethane, and methanol). Hexane partition was the most potent against MCF-7 cells growth with the lowest IC50 value. Then, it was subjected to two fractionation procedures, resulting in the identification of the CL bioactive fraction (II-F7) with potent toxicity against MCF-7 cells. **Results:** Further investigation into CL bioactive fraction (II-F7) revealed significant dose-dependent growth inhibitory effects on MCF-7 cells, which were attributed to the induction of apoptosis, as evidenced by the presence of apoptotic bodies, fragmented DNA, and disruption of mitochondrial membrane potential. Additionally, treatment with CL bioactive fraction (II-F7) upregulated the expression of pro-apoptotic genes (*DDIT3, GADD45G* and *HRK*) and significantly increased the activities of caspase-8 and caspase-9. **Conclusion:** Overall, this study suggests that bioactive fraction (II-F7) from CL extract has significant and selective cytotoxicity against MCF-7 cells through inducing apoptosis and has potential as a therapeutic agent for breast cancer treatment.

Keywords: breast cancer- cocoa leaf- bioactive- fractionation- apoptosis- gene expression- MCF-7

Asian Pac J Cancer Prev, **24 (7)**, 2473-2483

Introduction

Cancer is a multifactorial and heterogeneous disease, which arises from genetic and epigenetic alterations leading to the loss of cell cycle control, apoptosis, and senescence. These changes result in the abnormal proliferation and survival of cells that fail to respond properly to physiological signals and are not subject to normal growth constraints (Kamian et al., 2023). During cancer development, the activation of oncogenes and/or the inactivation of tumor suppressor genes, lead to uncontrolled cell growth and proliferation. Recent studies have highlighted the role of epigenetic mechanisms in oncogene activation, tumor suppressor gene inactivation, and genomic instability, which contribute to the development and progression of cancer (Cardoso et al., 2023). As cancer poses a significant burden on public health systems worldwide, there is a pressing need to develop effective strategies for prevention and treatment. According to the Global Cancer Observatory, cancer is projected to be responsible for approximately 11 million deaths globally in 2018, underscoring the urgent need for innovative approaches to combat this disease (The Global Cancer Observatory, 2018).

Breast cancer is a leading cause of mortality worldwide, with a growing number of cases diagnosed each year (Siegel et al., 2022). The use of surgery and chemotherapy has contributed to improved survival rates among patients with breast cancer (Hussain et al., 2022). However, traditional chemotherapeutic agents such as tamoxifen and cisplatin can cause significant side effects including anemia, alopecia, and nausea (Aljari et al., 2021). Thus, there is a pressing need for the development of natural and effective anticancer agents that can inhibit tumor growth without causing debilitating side effects. To this end, researchers are exploring the potential of novel compounds with selective anticancer properties as potential alternatives to traditional chemotherapy.

*[1]Department of Nutrition and Dietetics, College of Pharmacy, Al-Ain University, Abu-Dhabi, United Arab Emirates. [2]Faculty of Applied Sciences and Technology, Universiti Tun Hussein Onn Malaysia (UTHM)- Pagoh Campus, Johor, Malaysia. [3]Department of Biomedical Sciences, Faculty of Medicine and Health Sciences, Universiti Putra Malaysia, Serdang, 43400, Selangor, Malaysia. [4]Department of Clinical Nutrition, Faculty of Applied Medical Sciences, Al-Azhar University of Gaza, Gaza City, State of Palestine. [5]Sport and Exercises Sciences School, Faculty of Science, Liverpool John Moores University, Liverpool, UK. *For Correspondence: yazan.ranneh@aau.ac.ae*

Theobroma cacao (*T. cacao*) is known to contain numerous phytochemical compounds that have been demonstrated to have significant nutritional and therapeutic values (Acosta-Otálvaro et al., 2022). Among these compounds, polyphenolic compounds are found to be the most abundant in cocoa beans, whether they are dried or unfermented, contributing to around 13.5% of the tissue. The identification of a broad range of useful bioactive compounds has revolutionized the popular perception of cocoa as a mere stimulant or luxury food, as most identified active compounds have been found to exert different pharmacological effects in vitro and in vivo, with potential health implications (Dicks et al., 2018). Recently, the non-edible parts of *T. cacao* have been shown to contain a wide range of therapeutic phytochemical compounds. However, despite the increasing interest in the medicinal properties of *T. cacao*, the bioactive compounds and molecular mechanisms of cocoa leaf extract on MCF-7 cancer cells have not yet been fully understood. Following AIMRDA-Standard-Reporting-for-Anticancer Activity of Natural-Compounds-Tool (Ahmad et al., 2021), this study aims to identify the potent bioactive fraction of the methanolic crude extract from cocoa leaf (CL) and to evaluate its cytotoxic and apoptotic effects against the human breast cancer cell line with positive estrogen receptor (MCF-7).

Materials and Methods

Cocoa leaf extract preparation

Cocoa leaf (CL) was obtained from a cocoa smallholder field in Ranau, Sabah, Malaysia, during the peak fruiting season in April 2020. The plant material was identified and authenticated by a professional botanist (Dr. Alona Cuevas Linatoc) at the botanical laboratory of Universiti Tun Hussein Onn Malaysia, and a voucher specimen (No. 1182020CL) was assigned. Based on the method developed by Osman and colleagues (2004) with some adjustments, one kilogram of dried and ground CL was extracted by soaking in 10 liters of 70% methanol for three days at room temperature. The crude extract was filtered using Whatman filter paper, pooled, and concentrated using rotary evaporation at 40ºC to obtain a concentrated methanolic crude extract. The concentrated extract was then fractionated using a sequential liquid-liquid partitioning technique with hexane (250 mL), dichloromethane (250 mL), and methanol (250 mL) to produce three partitions. After filtration with rotary evaporation, the percentage yields of the crude extract and partitioned fractions were calculated as follows:

Yield (%) = Sample extract weight / Fresh plant part weight X 100

Bioassay guided fractionation

Avasthi et al. (2016) described a method for bioassay-guided isolation of a dried cocoa leaf (CL) extract, which was modified slightly for the current study. The aim of the purification process was to identify the most potent cytotoxic bioactive fraction against MCF-7 cells using MTT assay (Figure 1). Three partitions of the methanolic CL extract were obtained using liquid-liquid partitioning with different solvents: hexane, dichloromethane, and methanol. Based on the MTT assay results, the hexane partition was selected for further fractionation using flash column chromatography. Elution was performed using a series of solvent systems as follow; hexane (100.0% v/v), hexane: dichloromethane (4:1 v/v), hexane: dichloromethane (3:2 v/v), hexane: dichloromethane (2:3 v/v), hexane: dichloromethane (1:4 v/v), dichloromethane (100.0%), dichloromethane: methanol (4:1 v/v), dichloromethane: methanol (3:2 v/v), dichloromethane: methanol (2:3 v/v), dichloromethane: methanol (1:4 v/v) and methanol (100.0% v/v) and the bioactive constituents of each fraction were assessed using thin-layer chromatography (TLC) at 254 and 366 nm wavelengths to identify similar compounds for combination. Subsequently, all the fractions were concentrated by vacuum rotary evaporation at 40°C. Based on the lowest IC_{50} MTT assay results, the most potent bioactive fraction (II-F7) was selected for subsequent assays.

Cell viability assay

The estrogen receptor-positive human breast cancer cell line (MCF-7) was purchased from American Type Culture Collection (ATCC) and was cultured in RPMI 1640 medium containing 10% fetal bovine serum and a combination of 150 units/mL of penicillin-streptomycin (Invitrogen Co., Carlsbad, CA, USA) for optimal growth. The cells were maintained in a CO_2 incubator at 37°C. The cells were examined for mycoplasma contamination using EZ-PCR mycoplasma detection kit (InvivoGen, USA). The cells were seeded at a density of 2×10^3 cells per mL in a 96-well plate and allowed to adhere for 24 hours before treatment. The cells were treated with various concentrations (0.0001, 0.001, 0.01, 0.1, 1, 10, 100 µg/mL) of the bioactive fraction (II-F7) of the cocoa leaf extract, which was dissolved in 0.1% dimethyl sulfoxide (DMSO). After 24, 48, and 72 hours of incubation, the viability of the cells was assessed by their ability to metabolize 3-(4,5-dimethylthiazol-2-yl)-2,5-diphenyltetrazolium bromide (MTT) into formazan. The absorbance of the formazan was measured at 550 nm using a Versamax tunable reader (Molecular Devices, USA). Cell viability was calculated as a percentage of the control using the following formula:

$$\% \text{ cytotoxicity} = \frac{\text{Absorbance treated cells}}{\text{Absorbace control cells}} \times 100$$

Based on the results of the MTT assay, the dose-response curve was plotted and the 25%, 50% and 75% inhibitory concentrations (IC_{25}, IC_{50}, IC_{75}) of CL bioactive fraction (II-F7) were determined and were used in the remaining assays.

Morphological assessment of cells via phase contrast light and fluorescent microscope

A total of 1 x 10^5 cells/mL of MCF-7 cells were seeded in 96-well plate (BD Falcon, USA) with each well containing a volume of 200 µL. After incubating the cells for 24 hours at 5.0% CO_2 and 37°C, the cells were

treated with CL bioactive fraction (II-F7) at three different concentrations, namely IC_{25}, IC_{50}, and IC_{75} for 48 hours. The morphological changes of MCF-7 cells were observed under an inverted light microscope with phase-contrast at 10x and 20x magnification (Nikon, Minato City, Japan). In addition, MCF-7 cells were treated with 0.1% DMSO or three different concentrations of CL bioactive fraction (II-F7), followed by staining with 10 µL of 100 µg/mL acridine orange (AO) and 100 µg/mL of propidium iodide (PI) and incubated for 10 minutes at room temperature for fluorescent microscope observations. After washing the cells with PBS, slides were examined under fluorescent microscope (DM2500; Leica Microsystems, Germany) at 10x and 40x magnification using an excitation filter and barrier filter 450-490 nm and long pass filter 520 nm. The percentage of MCF-7 cells with pathological changes was manually calculated based on the observation of about 250 cells.

Mitochondrial membrane potential (MMP)

The MCF-7 cells were cultured in a 96-well amber plate (BD Falcon, USA) at a density of 1 x 105 cells/mL and incubated at 37°C and 5% CO_2 for 24 hours. Subsequently, the cells were treated with three different concentrations of CL bioactive fraction (II-F7), IC_{25}, IC_{50}, and IC_{75}, or 0.1% DMSO as a control, for 48 hours. After the cells were washed with PBS, 10 µL of JC-1 dye (Thermo Fisher, USA) was added to the cells and gently mixed according to the manufacturer's instructions. The cells were incubated at room temperature for 10-15 minutes and washed twice with PBS. The red and green fluorescence of the cells were measured using a fluorescence microplate reader at an excitation/emission wavelength of 485/595 nm.

Apoptosis assay

MCF-7 cells were cultured in a six-well plate at a density of 2×10^6 cells per well. Three different concentrations of CL bioactive fraction (II-F7) corresponding to IC_{25}, IC_{50}, and IC_{75} were added to the cells and incubated for 48 hours, while untreated cells were used as control. Subsequently, MCF-7 cells were treated with Muse Annexin V & Dead Cell Reagent (Millipore) following the manufacturer's protocol. The apoptosis profiles were then analyzed and obtained using a Muse cell analyzer (Millipore).

Determination of apoptotic marker (Caspase-3, -8 and -9)

After 24 hours of culturing MCF-7 cells at a density of 1 x 10^5 cells/mL in 96-well plates, three different concentrations (IC_{25}, IC_{50}, and IC_{75}) of CL bioactive fraction (II-SF7) or 0.1% DMSO were added to the cells. The cells were then incubated at 37 °C with 5% CO_2 for 48 hours. Following this incubation period, the cells were lysed using a cell extraction buffer that was mixed with a cocktail of protease inhibitors and phenyl methane sulfonyl fluoride. The levels of active caspase-3, caspase-8, and caspase-9 were quantified using commercially available sandwich ELISA kits from Fine Biotech (Shanghai, China), according to the manufacturer's instructions. The absorbance of the samples was measured at 405 nm using an ELISA reader (Asys UVM 340, UK). The experiments were conducted in triplicate to ensure statistical significance.

DNA fragmentation

MCF-7 cells at the density of 5 x 105 cells/mL seeded in 6-well plate to be grown in 24 h in an incubator with 5.0% CO_2 at 37°C. Then, MCF-7 cells were treated with 0.1% DMSO or three different concentrations of CL bioactive fraction (II-F7), IC_{25}, IC_{50} and IC_{75} for 48 h. Then, the treated cells were centrifuged at 2000 rpm for 5 min and the cell pellet was washed twice with PBS. Cayman DNA Laddering assay kit (Ann Arbor, Michigan) was used for DNA laddering analysis and a dry cell pellet was obtained according to the manufacturer instructions. After resuspending the dry pellet in 25 µL of Tris EDTA buffer, electrophoresis procedure was performed. After mixing 10 µL of MCF-7 cells extract with 2 µL of loading buffer, DNA fragment was separated in 0.8% agarose gel stained 5.0 mg/ml ethidium bromide at 75V for 65 min using an agarose gel electrophoresis system. The DNA fragment size was determined by using 1 kb of DNA ladder (Invitrogen, USA) as a marker. DNA fragmentations were seen under UV light using FluorChem 5500 Chemiluminescent (Alpha Innotech, USA).

Expression of apoptotic genes in MCF-7 cells

The Human Apoptosis Exprofile™ qPCR Arrays (GeneCopoeia, USA) was used according to the manufacturer guideline to study the gene expression of apoptosis-related genes in MCF-7 cells treated with CL bioactive fraction (II-F7) at IC_{50} and IC_{75}. The reagent of all-in-one qPCR Mix kit needed for the qPCR array were first thawed and inverted the tubes to mix gently. Then, the reagents were briefly centrifuged at 4000 rpm for 5 s to convey the substance to the base of the tubes and placed on ice. The plate sealing of the 96-well qPCR array was carefully peeled off after centrifuged at 4000 rpm for 5 s to discard any condensation that has gathered on the plate fixing surface. The mixture of 2x all-in-one qPCR mix (10 µL), cDNA with 10 times dilution (1 µL) and topped up with DEPC-168 treated water to make up a last volume of 20 µL, taking the manufacturer guideline. Then, the qPCR solution was mixed thoroughly and briefly centrifuged at 4000 rpm for 5 s. Exactly 20 µL mixed qPCR working solution was pipetted into each well and then qPCR reaction plate was sealed with new sealing film tightly. The plate was then quickly centrifuged to sediment all solutions at the bottom of the well. Real-time PCR was accomplished by using the qPCR instrument (Eppendorf Mastercycler® ep realplex). The plate was heated until 95°C for 10 minutes and followed by 40 cycles of 95ºC for 10 s (denaturation), 60ºC for 20 s (annealing) and 72ºC for 20 s (extension). The analysis of melting curve was conducted immediately after qPCR cycling by heated the plate at 95ºC for 10s with heating rate at 0.5ºC/unit time and followed by 25ºC for 30 s. The experiment was carried out in three replications, using three plates for each experimental sample. Table S1 and Table S2 include the positions of the human apoptotic genes in the 96 wells plate. The threshold cycle (Ct) value for

each gene expressed was determined as a relative value by normalization against the housekeeping gene of the GAPDH level and all the results were compared with those determined for the healthy controls. The relative gene expression level was measured using the $\Delta\Delta C_t$ method and the value was expressed as an n-fold change relative to the control.

Identification of chemical constituents in CL bioactive fraction (II/F7) using GC-MS

The chemical constituents of CL bioactive fraction (II-F7) were identified using gas chromatography-mass spectrometry (GC-MS), with modifications to the method described by Santa (Santa 2011). The GC-MS analysis was performed using a QP2010 Plus Shimadzu system, and a SGE BPX5 fused silica capillary column (30 m x 0.25 mm ID x 0.25 µm) with 100.0% dimethyl poly siloxane composition was used. An electron ionization system with ionizing energy of 70 eV was employed for GC-MS detection. Helium gas (99.999%) was used as the carrier gas at a constant flow rate of 1.5 mL/min, and the injection volume was 0.2 µL with a split ratio of 1.0. The injector temperature was set to 250ºC and the ion source temperature to 280ºC. The oven temperature was programmed from 50ºC (isothermal for 2 minutes) with an increase of 50ºC/minute to 200ºC, followed by an increase of 50ºC/minute to 320ºC, ending with a 9-minute isothermal at 320ºC. The mass spectra were obtained at 70 eV with a scan interval of 0.5 seconds and fragmented from 30 to 750 m/z. The GC run time was approximately 21 minutes. The relative % amount of each component was determined by comparing its average peak area to the total areas using mass spectra software and GC-MS chromatograms. The National Institute Standard and Technology (NIST) database, which contains more than 62,000 patterns, was used to interpret the mass spectra of the GC-MS. The mass spectrum of the unknown compound was compared with the spectrum of the known compound stored in the NIST library to identify the name, structure, and molecular weight of the components of the test materials.

Statistical analysis

All descriptive and inferential statistical analyses were presented as the mean ± standard error of the mean (SEM). The one-way analysis of variance (ANOVA) was applied for the statistical analysis, and comparison between groups was made using Tukey's test (SPSS version 17.0, SPSS Inc., USA) and p-value < 0.05 was considered statistically significant. The raw data of qPCR were analysed using GeneCopoeia's online data analysis system at http://www.genecopoeia.com/product/gene-qpcr-array/#Analysis_Tool. This data analysis system was used the $\Delta\Delta C_t$ method to perform fold-change analysis or simple statistical analysis of the expression level (C_t values) for each gene. The GPR fold change was calculated for each gene tested and data with $p < 0.05$ were deemed statistically significant. GPR uses the two-tailed unpaired Student's t-test to compare the normalized Cq values for each gene between control and experimental groups. All the experiments were performed in triplicate.

Results

CL bioactive fraction (II-F7) cytotoxicity against MCF-7 cells

The cytotoxic effects of CL bioactive fraction (II-F7) against MCF-7 cells were evaluated in a dose-dependent and time-dependent manner. The results revealed that at the highest concentration (100 µg/mL), the fraction inhibited over 50% of MCF-7 cells after 48 h and 72 h. The IC_{50} values of the fraction at 24, 48 and 72 hours were found to be 68.80 ± 5.76, 11.77 ± 1.39, and 41.01 ± 2.51 µg/mL, respectively. Therefore, a duration of 48 h was selected for further assays, with three different concentrations of IC_{25} (0.3 µg/mL), IC_{50} (6.4 µg/mL), and IC_{75} (45 µg/mL).

The cytotoxicity results were further validated by examining the morphological changes of MCF-7 cells using acridine orange and propidium iodide staining under light and fluorescence microscope. Propidium iodide binds with DNA and emits a red-orange color during apoptosis or necrosis, while acridine orange stains viable cells green. It was observed that the number of MCF-7 cells treated with CL bioactive fraction (II-F7) decreased in a dose-dependent pattern after 48 hours. The control MCF-7 cells remained stained green, indicating intact cells, while CL bioactive fraction (II-F7) treated cells showed apoptotic characteristics such as membrane blebbing and cell shrinkage. To quantify the percentage of cells undergoing early or late apoptosis or necrosis, random scoring was used. The results showed that the percentage of early apoptotic MCF-7 cells treated with IC_{75} of CL bioactive fraction (II-F7) for 48 hours was significantly higher ($P<0.05$) than those treated with IC_{50} and IC_{25}. This result was further corroborated by analyzing the mitochondrial membrane potential ΨΔm, which is an early marker for apoptosis. The incubation of MCF-7 cells with CL bioactive fraction (II-F7) for 48 hours caused a significant loss of mitochondrial membrane potential ΨΔm at IC_{75} and IC_{50}, where the red/green ratio emission from JC-1 dye was 45% and 51%, respectively.

Effect of CL bioactive fraction (II-F7) on apoptosis in MCF-7 cell

The results of the flow cytometry assay showed significant apoptotic changes in the MCF-7 cell profile after incubation with different concentrations (IC_{25}, IC_{50}, and IC_{75}) of the CL bioactive fraction (II-F7) for 48 hours, and the cells were stained with V-FTIC/propidium (Figure 3A). The IC_{50} and IC_{75} concentrations induced a significant ($P<0.05$) increase in both early and late apoptosis compared to the control group (Figure 3A and 3B). Specifically, the percentage of cells undergoing late apoptosis was 50% and 20% after exposure to IC_{75} and IC_{50}, respectively. Moreover, a further significant increment from 1.25% to 4.25% was observed when the cells were exposed to both IC_{50} and IC_{75} concentrations (Figure 3A and 3B). To further support the flow cytometry apoptotic results, the protein levels of caspase-3, caspase-8, and caspase-9 were detected using sandwich

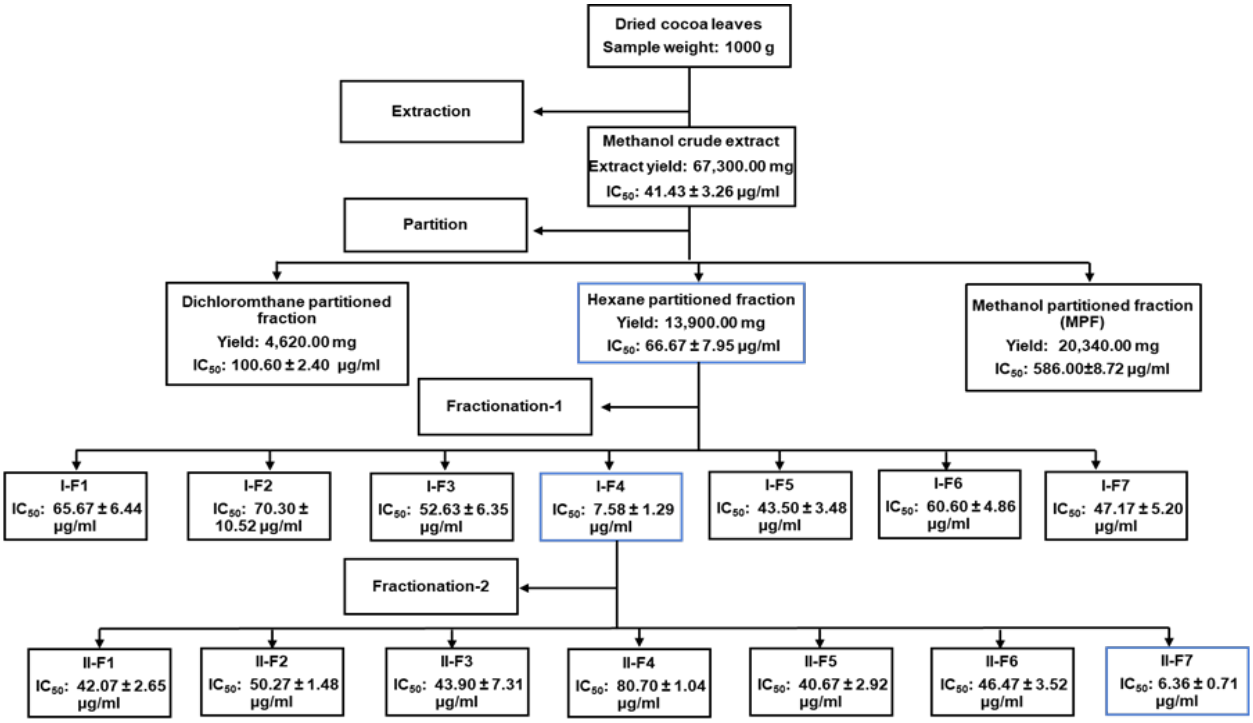

Figure 1. Scheme of Bioassay-Guided Fractionation Process of CL Crude Extract. Isolation of CL bioactive fraction (II-F7) were guided by the lowest IC50 of partition and fractionation extracts against MCF-7 cells with 48 hours incubation using MTT assay. Concentration of samples were carried out using a rotary evaporator. TLC results were applied to combine the similar fractions.

ELISA (Figure 3C). The fold changes of these apoptotic proteins induced by the CL bioactive fraction (II-F7) were compared to the control in MCF-7 cells. Surprisingly, IC_{25} of the CL bioactive fraction (II-F7) significantly ($P<0.05$) increased the caspase-3 levels, while both IC_{50} and IC_{75} had similar values. However, the levels of caspase-8 in MCF-7 cells were approximately similar for the three concentrations of CL bioactive fraction (II-F7), while IC_{50} and IC_{75} concentrations had a higher increment of caspase-9 than IC_{25} (Figure 3C).

The presence of DNA fragmentation is a key indicator of apoptotic cell death. In this study, we detected DNA fragmentation in MCF-7 cells exposed to CL bioactive fraction (II-F7) by extracting the genomic DNA of the

Table 1. GPR Fold Change of Selected Apoptosis-Related Gene Expression in MCF-7 Cells Treated with CL Bioactive Fraction (II-F7). Bold-face and italic indicates up-regulated and down-regulate of the selected gene expression in comparison with IC_{50} and IC_{75} concentration. Data represent the mean of samples induced fold change in gene expression relative to control-treated cells (n=3), $P < 0.05$.

Gen bank number	Gene name	Gene symbol	GPR Fold Regulation	
			IC_{50} (6.4 µg/ml)	IC_{75} (45.0 µg/ml)
1	BCL2-associated anthanogene 3	*BAG3*	3.47	7.48
2	BCL2-associated X protein	*BAX*	-3.31	-2.14
3	BCL2-like 1	*BCL2L1*	-1.76	-2.88
4	BCL2/adenovirus E1B 19kDA interacting protein 3	*BNIP3*	-3.77	-2.74
5	BCL2-related ovarian killer	*BOK*	-1.53	-2.84
6	Caspase recruitment domain family, member 10	*CARD10*	-1.19	-2
7	CD40 molecule, TNF receptor superfamily member 5 Clusterin	*CD40*	2.66	2.03
8	Clusterin	*CLU*	7.29	7.76
9	Death –associated protein	*DAP*	3.06	2.12
10	DNA-damage-induceble transcript 3	*DDIT3*	1.54	3.84
11	Transcription factor E2F1 (RBAP1; RBBP3; RBP3)	*E2F1*	-1.82	-2.25
12	Growth arrest and DNA-damage-inducible, gamma	*GADD45G*	1.66	6.73
13	Hara-kiri, BCL2 interacting protein (contains only BH3 domain)	*HRK*	-1.24	2.01
14	Heat shock 70 kDA protein 1A	*HSPA1A*	15.17	83.46

Table 2. The Chemical Composition of CL Bioactive Fraction (II-F7) by GC-MS Reported in Percentage of Similarity index (%), Molecular Weight (g) and Retention Time (min).

Compound	Formula	Area (%)	MW (g)	RT (min)
2-Butanone	C_4H_8O	1.1	72	4.017
2-Ethyl-2-butenal	$C_6H_{10}O$	0.9	98	4.018
2-Ethyl-2-butenal	$C_6H_{10}O$	1.21	98	4.325
6-Methyl-5-hepten-2-one	$C_8H_{14}O$	1.53	126	5.125
2-Methyl-6-methylene-2-octane	$C_{10}H_{18}$	0.78	138	5.667
(E)-3,7-Dimethyl-2,6-octadienal	$C_{10}H_{16}O$	0.5	152	5.758
2-Methylbenzaldehyde	C_8H_8O	0.98	120	6.042
1-Methyl-4-(2-methyloxiranyl)-7-oxabicyclo 4.1.0)heptane	$C_{10}H_{16}O_2$	1.2	168	6.542
4-(1-Methyl)-2-cyclohexane-1-one	$C_9H_{14}O$	2.3	138	6.75
2,4-Dimethyl-1-heptanol	$C_9H_{20}O$	0.45	144	6.883
9-Methyl-1-decene	$C_{11}H_{22}$	0.67	154	7.125
4-Propylbenzaldehyde	$C_{10}H_{12}O$	1.01	148	7.292
Lilac aldehyde	$C_{10}H_{18}O_2$	0.94	170	7.358
6,10-Dimethyl-5,9-undecadien-2-one	$C_{13}H_{22}O$	1.41	194	8.117
Oxalic acid	$C_{15}H_{28}O_4$	0.27	272	8.217
2,6-Bis(1,1-dimethylethyl)-2,5-cyclohexadiene-1,4-dione	$C_{14}H_{20}O_2$	0.31	220	8.258
Phenol,2,4-bis(1,1-dimethylethyl)	$C_{14}H_{22}O$	16.26	206	8.450
6,11-Dimethyl-2,6,10-dodecatrien-1-ol	$C_{14}H_{24}O$	0.57	208	8.525
Cyclohexanol, 2-methyl-3-(1-methylethenyl)-, acetate, (1.alpha.,2.alpha.,3.alpha.)	$C_{12}H_{20}O_2$	0.42	196	8.692
Methyl 12-methyltridecanoate	$C_{15}H_{30}O_2$	1.04	242	9.417
Cis-Z-alpha-bisabolene epoxide	$C_{15}H_{24}O$	0.54	220	9.900
7-Oxabicyclo[4.1.0]heptane, 1-methyl-4-(2-methyloxiranyl)	$C_{10}H_{16}O_2$	2.43	168	9.950
Hexadecanoic acid methyl ester	$C_{17}H_{34}O_2$	7	270	10.292
1-Oxa-spiro[4.5]deca-6,9-diene-2,8-dione, 7,9-di-tert-butyl-	$C_{17}H_{24}O_3$	0.29	276	10.342
Benzenepropanoic acid, 3,5-bis(1,1-dimethyl)-4-hydroxy-, methyl ester	$C_{18}H_{28}O_3$	1.05	292	10.383
4,8,12-Tetradecatrienal, 5,9,13-trimethyl	$C_{15}H_{26}O$	0.58	222	10.617
1-Nonadecanol	$C_{19}H_{40}O$	0.91	284	10.942
Phytol	$C_{20}H_{40}O$	0.49	296	11.025
Octadecanoic acid methyl ester	$C_{19}H_{38}O_2$	7.34	298	11.075
3-Ethoxy-3,7-dimethyl-1,6-octadiene	$C_{12}H_{22}O$	1.2	182	11.392
Hexadecanoic acid-2-hydroxyethyl ester	$C_{18}H_{36}O_3$	4.2	300	11.533
3-Chloropropionic acid	$C_{20}H_{39}ClO_2$	0.57	346	11.692
4,8,12,16-Tetramethylheptadecan-4-olide	$C_{21}H_{40}O_2$	0.91	324	11.950
Octadecanoic acid-2-hydroxyethyl ester	$C_{20}H_{40}O_3$	2.39	328	12.225
Glycidyl stearate	$C_{21}H_{40}O_3$	1.05	340	12.408
Mono(2-ethylhexyl) phthalate	$C_{16}H_{22}O_4$	0.75	278	12.525
Hexadecanoic acid-2-hydroxy-1-(hydroxymethyl)ethyl ester	$C_{19}H_{38}O_4$	1.45	330	12.492
Octadecanoic acid-2,3-dihydroxyprophyl ester	$C_{21}H_{42}O_4$	0.43	358	13.125
Unknown	-	33.08	-	17.216

cells. Gel electrophoresis of the extracted DNA revealed the formation of a DNA ladder in the treated cells, which was not observed in the untreated cells. Specifically, IC_{50} and IC_{75} concentrations of CL bioactive fraction (II-F7) caused significant DNA fragmentation in the treated MCF-7 cells. To investigate the role of CL bioactive fraction (II-F7) in MCF-7 cell apoptosis, we conducted quantitative real-time PCR analysis of the treated cells. Our results showed changes in the expression of apoptotic genes in response to treatment with IC_{50} and IC_{75} concentrations of CL bioactive fraction (II-F7) for 48 hours. The expression of seven genes was altered at IC_{50}, while 14 genes were altered at IC_{75}. In particular, the *BAX* and *BNIP3* genes were down-regulated and five genes (*BAG3*, *CD40, CLU, DAP,* and *HSPA1A)* were up-regulated at the IC_{50} concentration. At the IC_{75} concentration, six genes (*BAX*, *BCL2L1, BNIP3, BOK, CARD10*, and *E2F1*) were down-regulated, while eight genes (*BAG3*, *CD40, CLU, DAP, DDIT3, GADD45G, HRK*, and *HSPA1A*) were up-regulated. These findings suggest that CL bioactive fraction (II-F7) induces apoptosis in MCF-7 cells by regulating the expression of

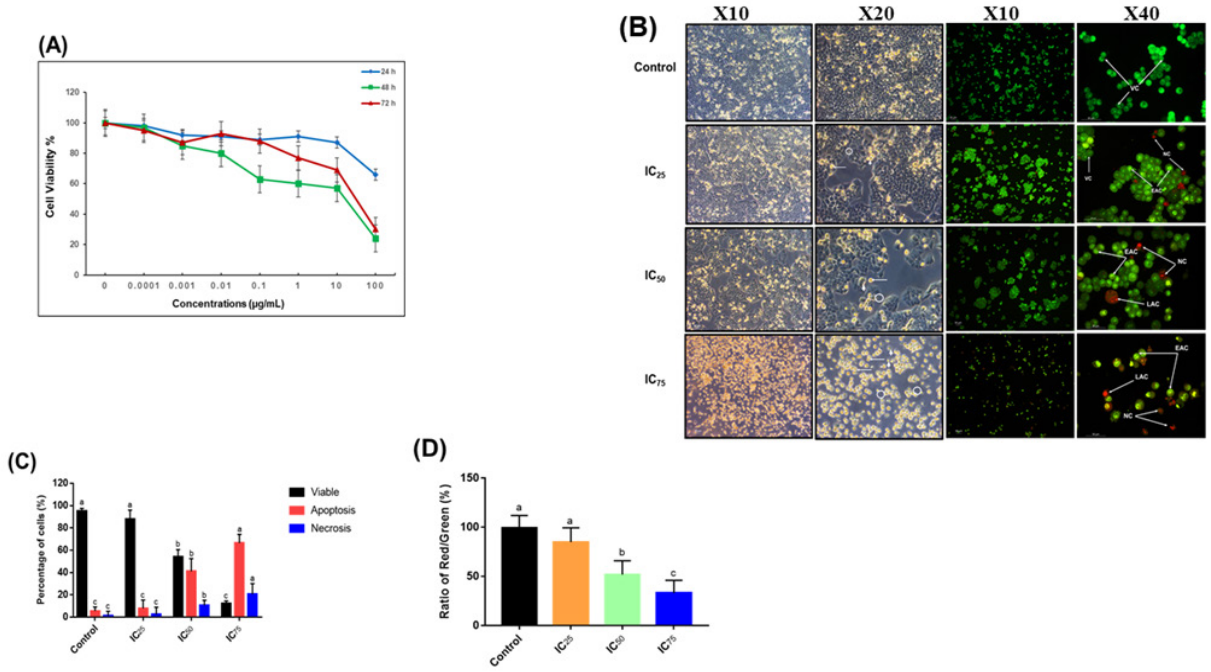

Figure 2. CL Bioactive Fraction (II-F7) Inhibit MCF-7 Proliferation. (A) Cell viability percentage of MCF-7 cells-treated with serial concentrations of CL bioactive fraction (II-F7) at 24 h, 48 h, and 72 h. (B) phase contrast micrograph of light and fluorescence microscope for MCF-7 cells treated with three concentrations (IC_{25}, IC_{50}, IC_{75}) of CL bioactive fraction (II-F7) for 48 h. Under light microscope, the treated cells show apoptotic bodies (circle), cell shrinkage (arrow) and membrane blebbing (head arrow). The fluorescence micrographs show untreated cells with normal structure (intact green) while the treated cells show early apoptosis (bright green), late apoptosis (dark orange) and necrotic cells (bright red). VC: viable cells, EAC: early apoptotic cells, LAC: late apoptotic cells, NC: necrotic cells. Figures were obtained from three independent experiments with similar parameters. (C) Percentage of viable, apoptotic, and necrotic of MCF-7 cells following 48 hours treatment with CL sub-fraction (II/SF7) at concentrations of IC_{25}, IC_{50} and IC_{75}. (D) ΨΔm changes in MCF-7 cells treated with three concentrations of CL bioactive fraction (II-F7) for 48 h and stained with JC-1. Values are the means of triplicate samples (n = 3). Data are presented as the mean ± SEM. Superscript letters indicate significant difference according to One-way ANOVA and Tukey honest significant difference test ($P<0.05$).

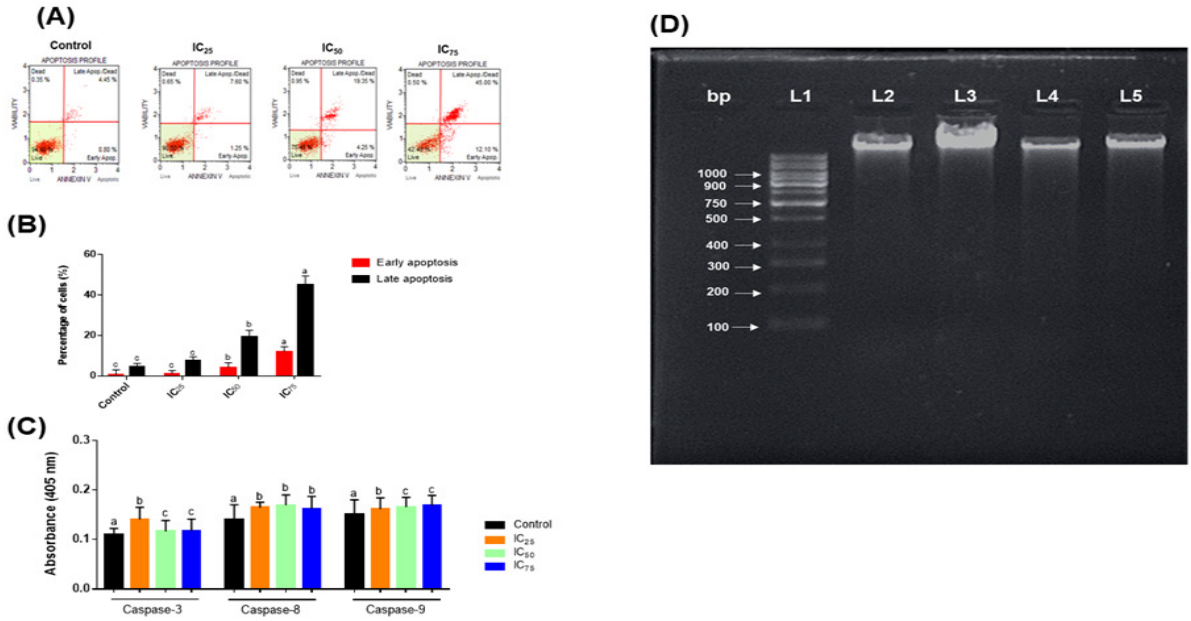

Figure 3. CL Bioactive Fraction (II-F7) Induce Apoptosis in MCF-7 Cells. (A) flow cytometry profile of MCF-7 cells treated with three concentrations (IC_{25}, IC_{50}, IC_{75}) of CL bioactive fraction (II-F7) for 48 h and stained with propidium iodide (PI). (B) percentage of MCF-7 cells undergoing late and early apoptosis. (C) levels of Caspase-3, -6, and -9 in MCF-7 cells after 48 h of treatment with three concentrations (IC_{25}, IC_{50}, IC75) of CL bioactive fraction (II-F7). (D) Apoptotic DNA fragmentation in MCF-7 cells following 48 hours treatment with CL bioactive fraction (II-F7) at concentrations of IC25, IC50 and IC75. L1: DNA size marker, L2: untreated cells (control), L3: IC_{25}, L4: IC_{50}, L5: IC_{75}. Values are the means of triplicate samples (n = 3). Data are presented as the mean ± SEM. Superscript letters indicate significant difference according to One-way ANOVA and Tukey honest significant difference test ($P<0.05$).

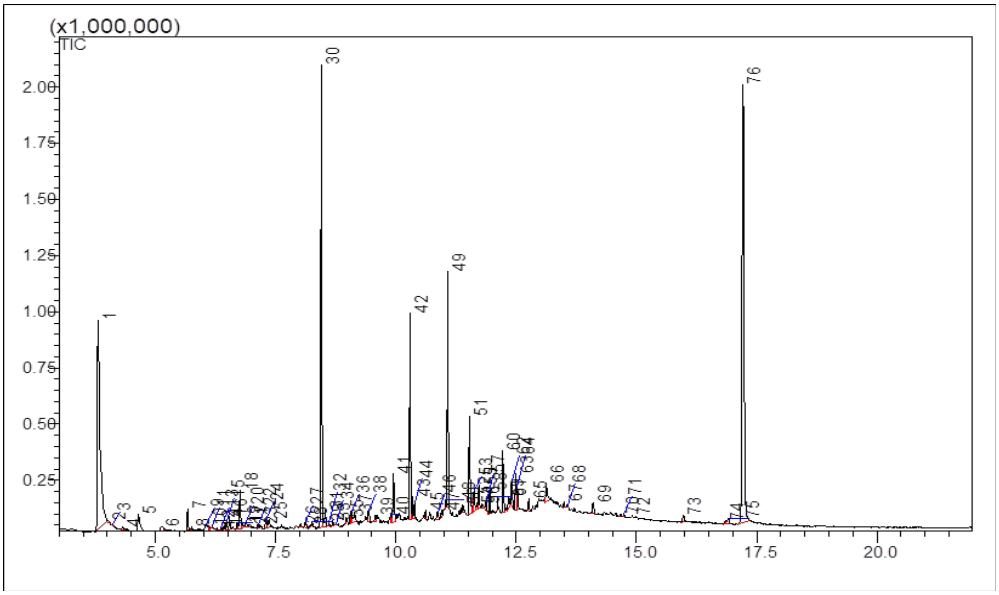

Figure 4. GC-MS Mass Spectral Profile of CL Bioactive Fraction (II-F7).

apoptotic genes.

Chemical constituent of CL bioactive fraction (II-F7)

Through the use of gas chromatography-mass spectrometry (GC-MS) and a thorough analysis of the NIST database, the active ingredients responsible for the potent cytotoxic effects of CL bioactive fraction (II-F7) have been identified and characterized. A visual representation of the GC-MS chromatogram in Figure 4 reveals that no less than 39 bioactive compounds were identified in the fraction. Notably, a group of nine major compounds were discovered to have a high percentage of area (>1.0%) within the fraction and were deemed significant in contributing to the observed cytotoxicity. These compounds include dimethyl sulfone, 4-(1-methyl)-2-cyclohexane-1-one, phenol-2,4-bis (1,1-dimethylethyl), 7-oxabicyclo[4.1.0] heptane-1-methyl-4-(2-methyloxiranyl), hexadecanoic acid methyl ester, octadecanoic acid methyl ester, hexadecanoic acid-2-hydroxyethyl ester, octadecanoic acid-2-hydroxyethyl ester, hexadecanoic acid-2-hydroxy-1-(hydroxymethyl) ethyl ester, and an unidentified compound (unknown) that accounts for a significant 33.08% of the fraction's composition.

Discussion

Recently, scientific literature has highlighted the significance of discovering alternative anti-cancer agents from natural sources. Cocoa, a rich source of high-quality polyphenols including catechins (29%-38% of total polyphenols), anthocyanin (4% of total polyphenol), and proanthocyanins (58%-65% of total polyphenols), has been extensively studied for its anti-cancer properties with promising results (Acosta-Otálvaro et al., 2022; Maskarinec, 2009). However, a comprehensive isolating method is required to identify the lead anti-cancer agent from the phytochemical matrix (Manzoor et al., 2019). In this study, a biological activity guided fractionation method was employed on CL using a sequential approach to investigate the anti-proliferative activities against MCF-7 cells. Hexane partitioning was used followed by two subsequent fractionations (Figure 1). The sequential fractionation method minimizes the side effects associated with crude extracts used for cancer therapy. The CL bioactive fraction (II-F7) with the lowest IC_{50} against MCF-7 cells was selected to determine the earliest time-point of cytotoxicity, which was 48 hours (Figure 2A). Similarly, Avasthi et al. (2016) fractionated Nepeta longibracteata Bentham extract and examined its efficacy against oxidative stress in human red blood cells.

The CL-bioactive fraction (II-F7) induced cellular shrinkage and membrane blebbing in MCF-7 cells, indicating apoptosis induction (Figure 2B). With increased concentrations of CL bioactive fraction (II-F7), the percentage of cells undergoing early apoptosis and necrosis also increased (Figure 2C). Krstic et al. (2015) reported cell rounding and detachment in HeLa cells treated with cocoa polyphenol extract for 24 hours, while Zeng and his colleagues (2017) observed apoptotic morphological changes in MCF-7 cells treated with epigallocatechin-3-gallate (EGCG) and catechin extracted from green tea. Moreover, HPLC analysis showed that the CL extract contained 1.78 mg/100 mg of EGCG and 7.69 mg/100 mg of catechin (Hassan and Swet Fan, 2005). The presence of high-quality polyphenols in similar amounts in the CL extract may account for the biological effect of CL bioactive fraction (II-F7) in modulating the morphological characteristics of MCF-7 cells by activating apoptotic pathways.

Apoptosis is a physiological process of programmed cell death that is known to be dysregulated in cancer (Mahassni and Al-Reemi, 2013). One of the earliest intracellular events that occurs during apoptosis is the disruption of mitochondrial membrane potential ($\Delta\Psi m$). To evaluate the effects of CL bioactive fraction (II-F7) on $\Delta\Psi m$ in MCF-7 cells, we used the mitochondria-specific cationic dye JC-1, which fluoresces red in polarized

mitochondria and green in depolarized mitochondria (Ansil et al., 2014). Treatment with CL bioactive fraction (II-F7) resulted in a dose-dependent depolarization of the mitochondrial membrane, as indicated by a decreased red/green fluorescence intensity ratio and a lower monomer-to-aggregate ratio (Figure 2D), suggesting that apoptosis was induced via the mitochondrial pathway. Similar depolarization of the mitochondrial membrane has been observed in MDA MB-231 cells treated with pentameric procyanidin extracted from cocoa at a concentration of 100 µg/ml (Ramljak et al., 2005).

Apoptosis is a cellular process that occurs through two pathways, namely the death receptor pathway and the mitochondrial pathway. While caspase-8 mediates the death receptor pathway and caspase-9 mediates the mitochondrial pathway, both pathways activate the effector caspase (caspase-3), ultimately resulting in apoptosis (Abotaleb et al., 2019). Previous studies have shown that cocoa procyanidin extract induces apoptosis in epithelial cell lines (OAW42 and OVCAR3) by activating caspase-3 (Taparia and Khanna, 2016). In this study, we demonstrated that CL bioactive fraction (II-F7) treatment in MCF-7 cells resulted in the activation of caspase-3, caspase-8, and caspase-9 (Figure 3C). The observed pattern of caspase activation suggests that CL bioactive fraction (II-F7) triggers both the mitochondrial and the death receptor pathways simultaneously. Furthermore, caspase-3 is responsible for cleaving poly(ADP-ribose) polymerase (PARP) and deactivating its DNA-repairing abilities during apoptosis, leading to DNA fragmentation (Alshabi et al., 2022). The DNA fragments of MCF-7 cells treated with IC_{75} (45.0 µg/mL) of CL bioactive fraction (II-F7) were visualized on the agarose gel with a ladder-like pattern of DNA fragments approximately 180–200 bp in size. Our results are consistent with Choi et al.'s findings (2022), where cocoa husk bean fractions induced DNA fragmentation in prostate cancer cells (PC3 and DU145) at a concentration of 200 µg/mL.

Apoptosis, a complex biological process that unfolds over multiple stages, is accompanied by a diverse array of changes. While much remains to be elucidated about the intricacies of this process, researchers have identified a handful of genes that play pivotal roles in regulating apoptosis, including the Bcl-2 family, C-myc, TNFR family, caspase family, and P53 (Abotaleb et al., 2019). In the present study, we investigated the impact of the CL bioactive fraction (II-F7) on apoptosis-related gene expression in MCF-7 cells. Our findings revealed that, of the genes examined, only three pro-apoptotic genes - *DDIT3, GADD45G,* and *HRK* - were differentially expressed in response to treatment with IC_{75} (45.0 µg/mL) of the bioactive fraction, with up-regulation of 3.8-, 6.73-, and 2.01-fold, respectively. Intriguingly, we also observed significant up-regulation of two anti-apoptotic genes, *BAG3* and HSPA1A, with fold-changes of 7.48 and 83.46, respectively (Table 1). Notably, the remaining genes - including *BAX*, *BCL2L1, BNPIP3, BOK, CARD10, CD40, CLU, DAP,* and *E2F1* - exhibited no significant changes in expression compared to the normal control group following treatment with IC_{50} (6.4 µg/mL) and IC_{75} (45.0 µg/mL) of the bioactive fraction.

The *DDIT3* gene, also known as *GADD153* or *CHOP*, encodes a transcription factor that belongs to the CCAAT/enhancer binding protein (C/EBP) family (Xavier et al., 2018). Upon activation, *DDIT3* plays a pivotal role in promoting the up-regulation of key signaling molecules that regulate the endoplasmic reticulum (ER) stress response and DNA damage response, inducing cell cycle arrest and apoptosis by halting progression from G1 to S phase (Lin et al., 2020). Interestingly, we found that the *DDIT3* gene was up-regulated in MCF-7 cells, as compared to the normal control group (Table 1). Furthermore, previous research has shown that the combination of *EGCG* and celecoxib treatment also up-regulated the *DDIT3* gene (Suganuma et al., 2011).

GC-MS is one of the analytical chemical approaches to identify bioactive compounds in crude botanical extracts, depending on the retention time and molecular weight, to formulate new potent drugs. Using this modern analytical technique, CL bioactive fraction (II-F7) contain significant compounds belonging to different classes. While 39 compounds were identified in this fraction, some of the compounds have potent biological activities. Phenol,2,4-bis(1,1-dimethylethyl) has been reported previously to have anti-bacterial, antioxidant and anti-inflammatory activities (Wagay et al., 2021). Octadecanoic acid methyl ester, identified in the chloroform extract of Achyranthes ferruginea demonstrated a cytotoxic activity against cervical cancer cell lines (Reza et al., 2021). Hexadecanoic acid methyl ester, Hexadecanoic acid-2-hydroxyethyl ester, Octadecanoic acid-2-hydroxyethyl, Methyl 12-methyltridecanoate have exhibited a broad spectrum of beneficial biological properties including toxicity towards cancer cells (Sheela and Uthayakumari, 2013; D and Arumugam, 2014; Abdel-Hady et al., 2018). The combination of several bioactive compounds in CL bioactive fraction (II-F7) support its potency against MCF-7 cancer cell line and pave the way for further research efforts to identify the mainly responsible compounds (Table 2).

In conclusion, our study has established that the CL bioactive fraction (II-F7) possesses potent anti-proliferative properties against the MCF-7 breast cancer cell line, likely attributable to its ability to trigger apoptosis. Specifically, our findings suggest that this effect may be mediated, at least in part, by the up-regulation of key apoptotic genes, including *DDIT3*, *GADD45G,* and *HRK*. Notably, we observed evidence of DNA fragmentation, mitochondrial membrane depolarization, and an increased proportion of cells undergoing both early and late apoptosis, all of which suggest the induction of apoptosis as the underlying mechanism of action. Additionally, our GC-MS analysis revealed the presence of 31 compounds within the bioactive fraction, which may contribute to its overall efficacy. However, further research is needed to evaluate the safety and therapeutic potential of the CL bioactive fraction (II-F7) across a broader range of cancer cell types and animal models, as well as to elucidate the specific molecular pathways involved in its apoptotic effects.

Abbreviations

CL; cocoa leave, GC-MS; Gas chromatography mass spectroscopy, FCC; Flash column chromatography, SAPK; stress-activated protein kinase, MAPK/ERK; mitogen-activated protein kinase/extracellular signal-regulated kinase.

Author Contribution Statement

Y.R, and M.F.A.B designed the study. A.M.A, Z.B.B, M.S.E and A.F carried out the date collection. Y.R, A.M.A and A.F conducted data analysis. Y.R and M.F.A.B conducted data interpretation, wrote and edited the manuscript. .

Acknowledgements

The authors would like to thank Al Ain University, Universiti Tun Hussein Onn Malaysia, and the Universiti Putra Malaysia (UPM) Department of Biomedical Sciences for providing human cancer cell lines, and laboratory facilities.

Availability of data

The data supporting the findings of this study are available from the corresponding author upon.

Conflict of interest

The authors herewith declare no conflict of interest, financial or otherwise.

References

Abdel-Hady H, Ahmed El-Wakil E, Abdel-Gawad M (2018). GC-MS Analysis, Antioxidant and Cytotoxic Activities of Mentha spicata. *Eur J Med Plants*, **26**.

Abotaleb M, Samuel SM, Varghese E, et al (2019). Flavonoids in cancer and apoptosis. *Cancers (Basel)*, **11**, 28.

Acosta-Otálvaro E, Valencia-Gallego W, Mazo-Rivas JC et al (2022). Cocoa extract with high content of flavan 3-ols, procyanidins and methylxanthines. *J Food Sci Technol*, **59**, 1152-61.

Ahmad R, Riaz M, Aldholmi M, et al (2021). Development of a Critical Appraisal Tool (AIMRDA) for the Peer-Review of Studies Assessing the Anticancer Activity of Natural Products: A Step towards Reproducibility. *Asian Pac J Cancer Prev*, **22**, 3735–40.

Aljari SM, Abutaha N, Ahmed Al-Keridis L, Abdullah Al-Doaiss A (2021). Acute and subacute toxicity studies of a new herbal formula induced apoptosis in the highly metastatic MDA-MB-231 cells. *J King Saud Univ Sci*, **33**, 101646.

Alshabi AM, Alkahtani SM, Shaikh IA, et al (2022). Phytochemicals from Corchorus olitorius methanolic extract induce apoptotic cell death via activation of caspase-3, anti-Bcl-2 activity, and DNA degradation in breast and lung cancer cell lines. *J King Saud Univ Sci*, **34**, 102238.

Ansil PN, Wills PJ, Varun R, Latha MS (2014). Cytotoxic and apoptotic activities of Amorphophallus campanulatus (Roxb.) Bl. tuber extracts against human colon carcinoma cell line HCT-15. *Saudi J Biol Sci*, **21**, 524–31.

Avasthi AS, Bhatnagar M, Sarkar N, Kitchlu S, Ghosal S (2016). Bioassay guided screening, optimization and characterization of antioxidant compounds from high altitude wild edible plants of Ladakh. *J Food Sci Technol*, **53**, 3244-52.

Cardoso Y, Resque RL, Yoshio D, et al (2023). Association between the Arg72Pro Genotypes in the TP53 Gene and Ile655Val in the HER2 Gene and the Risk of Developing Breast Cancer in the Population of Amapá, Northern Brazil. *Asian Pac J Cancer Prev*, **24**, 157–62.

Choi J, Yang C, Lim W, Song G, Choi HY (2022). Antioxidant and apoptotic activity of cocoa bean husk extract on prostate cancer cells. *Mol Cell Toxicol*, **18**.

Arumugam S (2014). GC – MS Analysis of Ethanol Extract of Cyperus rotundus Leaves. *Int J Curr Biotechnol*, **2**.

Dicks L, Kirch N, Gronwald D, et al (2018). Regular Intake of a Usual Serving Size of Flavanol-Rich Cocoa Powder Does Not Affect Cardiometabolic Parameters in Stably Treated Patients with Type 2 Diabetes and Hypertension—A Double-Blinded, Randomized, Placebo-Controlled Trial. *Nutrients*, **10**, 1435.

Hassan O , Swet Fan L (2005). The anti-oxidation potential of polyphenol extract from cocoa leaves on mechanically deboned chicken meat (MDCM). *LWT Food Sci Technol*, **38**.

Hussain N, Mahmood N, Anjum Nasim S, et al (2022). Targeting FoxP3 gene to check out the impairment of tolerance in breast cancer patients. *J King Saud Univ*, **34**, 101864.

Kamian S, Ashoori H, Vahidian F, Vahidian F (2023). The Relevance of Common K-RAS Gene Mutations and K-RAS mRNA Expression with Clinicopathological Findings and Survival in Breast Cancer. *Asian Pac J Cancer Prev*, **24**, 909–14.

Krstic M, Marija S, Katarina S, et al (2015). The anti-cancer activity of green tea, coffee and cocoa extracts on human cervical adenocarcinoma HeLa cells depends on both pro-oxidant and anti-proliferative activities of polyphenols. *RSC Adv*, **5**.

Lin H, Liu S, Gao W, et al (2020). *DDIT3* modulates cancer stemness in gastric cancer by directly regulating CEBPβ. *J Pharm Pharmacol*, **72**.

Mahassni SH, Al-Reemi RM (2013). Apoptosis and necrosis of human breast cancer cells by an aqueous extract of garden cress (Lepidium sativum) seeds. *Saudi J Biol Sci*, **20**, 131–9.

Manzoor MF, Ahmad N, Ahmed Z, et al (2019). Novel extraction techniques and pharmaceutical activities of luteolin and its derivatives. *J Food Biochem*, **43**.

Maskarinec G (2009). Cancer protective properties of cocoa: a review of the epidemiologic evidence. *Nutr Cancer*, **61**, 573–9.

Osman H, Nasarudin R, Lee S (2004). Extracts of cocoa (*Theobroma cacao* L.) leaves and their antioxidation potential. *Food Chem*, **86**.

Ramljak D, Romanczyk LJ, Metheny-Barlow LJ, et al (2005). Pentameric procyanidin from *Theobroma cacao* selectively inhibits growth of human breast cancer cells. *Mol Cancer Ther*, **4**, 537–46.

Reza ASMA, Haque MA, Sarker J, et al (2021). Antiproliferative and antioxidant potentials of bioactive edible vegetable fraction of Achyranthes ferruginea Roxb. in cancer cell line. *Food Sci Nutr*, **9**, 3777-805.

Sheela D, Uthayakumari F (2013). GC-MS analysis of bioactive constituents from coastal sand dune taxon- \textit{Sesuvium portulacastrum} (L.). *Biosci Discov*, **4**.

Siegel RL, Siegel MPH, Kimberly D, et al (2022). Cancer statistics, 2022. *CA Cancer J Clin*, **72**.

Suganuma M, Saha A, Fujiki H, et al (2011). New cancer treatment strategy using combination of green tea catechins and anticancer drugs. *Cancer Sci*, **102**.

Taparia SS , Khanna A (2016). Procyanidin-rich extract of natural

cocoa powder causes ROS-mediated caspase-3 dependent apoptosis and reduction of pro-MMP-2 in epithelial ovarian carcinoma cell lines. *Biomed Pharmacother*, **83**,130-40.

The Global Cancer Observatory (2018). All Cancers. Globocan.

Wagay NA, Rafiq S, Rather MA, et al (2021). Secondary metabolite profiling, anti-inflammatory and hepatoprotective activity of neptunia triquetra (Vahl) benth. *Molecules*, **26**, 7353.

Xavier MA, de Oliveira MT, Baranoski A, Mantovani MS (2018). Effects of folic acid on the antiproliferative efficiency of doxorubicin, camptothecin and methyl methanesulfonate in MCF-7 cells by mRNA endpoints. *Saudi J Biol Sci*, **25**.

Zeng L, Yan J, Luo L, Ma M, Zhu H (2017). Preparation and characterization of (-)-Epigallocatechin-3-gallate (EGCG)-loaded nanoparticles and their inhibitory effects on Human breast cancer MCF-7 cells. *Sci Rep*, **7**.